Electronic origin of the phase transition in ternary alloy Mo (Si 1 − x , Al x) 2

Zhengzheng Chen, Bin Shan, and Rong Chen

Citation: Applied Physics Letters **98**, 101903 (2011); doi: 10.1063/1.3562593
View online: http://dx.doi.org/10.1063/1.3562593
View Table of Contents: http://scitation.aip.org/content/aip/journal/apl/98/10?ver=pdfcov
Published by the AIP Publishing

Electronic origin of the phase transition in ternary alloy $Mo(Si_{1-x},Al_x)_2$

Zhengzheng Chen,[1] Bin Shan,[1,a)] and Rong Chen[2,b)]
[1]*State Key Laboratory of Material Processing and Die and Mould Technology, Huazhong University of Science and Technology, Wuhan 430074, Hubei, People's Republic of China and School of Materials Science and Engineering, Huazhong University of Science and Technology, Wuhan 430074, Hubei, People's Republic of China*
[2]*State Key Laboratory of Digital Manufacturing Equipment and Technology, Huazhong University of Science and Technology, Wuhan 430074, People's Republic of China and Department of Mechanical Engineering, Huazhong University of Science and Technology, Wuhan 430074, Hubei, People's Republic of China*

(Received 4 January 2011; accepted 15 February 2011; published online 7 March 2011)

The structural stability of the ternary alloy $Mo(Si_{1-x},Al_x)_2$ with different x has been investigated using first-principles pseudopotential plane wave method. The electronic origin of the $C11_b \rightarrow C40$ phase transition is revealed by analyzing the density of states and d-band splitting induced by the crystal field. We further propose the feasibility of controlling the microscopic structure by adding a quaternary component according to the mechanism presented in this work. © *2011 American Institute of Physics*. [doi:10.1063/1.3562593]

In recent years, $MoSi_2$ has attracted much attention as a potential candidate for high-temperature materials because of its excellent properties, such as high melting point (2293 K), low density, and oxidation resistance. The most severe impediment for the structural application of $MoSi_2$ is the pest disintegration around 780 K.[1,2] Many experiments[3–8] have shown that alloying with Al can significantly improve the resistivity of $MoSi_2$ toward the pest disintegration. Al substitution can also improve the structural toughness at low-temperatures, making $Mo(Si_{1-x},Al_x)_2$ a suitable alloy for turbine blades or coating. Recently, Pankhurst *et al.*[9] observed that when the concentration of Al in $Mo(Si_{1-x},Al_x)_2$ is beyond 10 at. %, the crystal structure transforms from the $C11_b$ to the $C40$ structure. Several other works also reported the effects of ternary and quaternary addition on controlling the structure of $MoSi_2$.[10–13] Despite extensive experimental efforts, an in-depth understanding of the mechanism driving the structural transition is still lacking. In the present work, we reveal the microscopic mechanism of the phase transition in $MoSi_2$ due to Al-doping using first-principles calculations.

The first-principles calculations were carried out using VASP package[14] with Perdew and Wang[15] exchange correlation functional and an energy cutoff of 350 eV. To compare the stability of both structures of $Mo(Si_{1-x},Al_x)_2$ with different x, a $3\times1\times1$ supercell of $C11_b$ and a $2\times1\times1$ supercell of $C40$ were employed (shown in Fig. 1). Three Al concentrations, $x=0$, 8.3, and 16.7 at. %, were considered. In the case of $x=16.7$ at. %, we have considered all the configurations in which two Al atoms substitute different Si sites, and the configuration with the lowest energy is taken as the ground-state. A $5\times10\times7$ k- mesh is adopted following the Monkhorst–Pack scheme.[16] The whole structure was allowed to relax until the force on each atom is less than 0.02 eV/Å. Our convergence test showed that the total energies is better than 1 meV/atom.

We begin our discussion by noting the rules for site occupancy of Al in two phases with $x=16.7$ at. %. Two quantities are taken to characterize the dopant distribution: the nearest distance between the two Al atoms, and the number of Al–Al pairs with distance shorter than a given R_{cut}(=4.5 Å), which is slightly larger than the third nearest neighbor Al–Al distance in $C11_b$ and the fifth nearest neighbor Al–Al distance in $C40$, respectively. The results are listed in Table I. In the $C11_b$ case, the structure prefers longer "nearest distance" and fewer "number of Al–Al pairs," which indicates a uniformly and sparse distribution of Al in $MoSi_2$. In contrast, there is no clear trend for favorable site occupancy of Al in $C40$ structure. Generally speaking, the average distance between the Al–Al pair is smaller in $C40$ than that in $C11_b$.

The lattice constant of each structure expands with the increasing x due to the larger radius of Al atoms compared to Si atoms. pV term is, however, ignored since the relative difference of volumes of supercells of $C11_b$ and $C40$ structures is smaller than 0.6% with the same x. Further, $C40$ was observed to be the ground state due to the Al substitution at room temperature.[9] And the difference of vibrational free energies between $C40$ and $C11_b$ $\Delta F_{vib}^{C40-C11_b}$ is estimated as 26 meV at 300 K in the present work. These two facts suggest ignoring vibrational entropy will not change our conclusions. We thus focus on the total energy (E) for the rest of the paper. Figure 2 shows the total energy curves of two structures with different x. E_{C11_b} and E_{C40} both rise with increasing substitution of Al, and the effect on $C11_b$ structure is

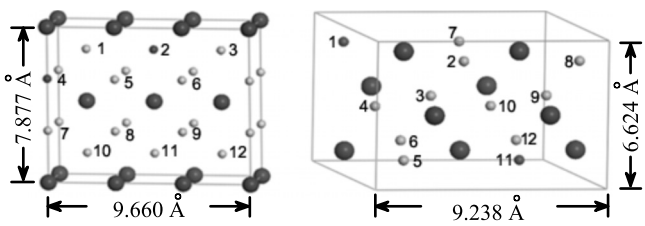

FIG. 1. $3\times1\times1$ $C11_b$ supercell (left) and $2\times1\times1$ $C40$ supercell (right). Dark large circles and light small circles represent Mo and Si atoms, respectively. Dark small circles indicate the lowest-energy positions for Al substitution. Lattice sites are marked by Arabic numerals 1–12.

a)Electronic mail: bshan@mail.hust.edu.cn.
b)Electronic mail: rongchen@mail.hust.edu.cn.

TABLE I. The total energies with different occupation position of Al. The abbreviation "Num" means "the number of Al–Al pairs with distance shorter than R_{cut}" and "Dis" means "the nearest distance of Al–Al pair," respectively. In each case, the ground energy is set as zero.

(a) $C11_b$ case			
Al-occupying site	Dis (Å)	Num	E_{tot} (meV)
1, 10	2.616	3	125
1, 4	2.616	2	57
1, 2	3.204	1	43
1, 7	4.531	0	37
2, 4	5.231	0	0
(b) $C40$ case			
1, 6	2.566	2	125
1, 9	2.566	1	121
1, 2	2.686	1	51
1, 5	3.219	1	43
1, 8	2.622	2	26
1, 10	4.565	0	19
1, 11	3.166	1	0

more substantial. In the case of $x=0$ at. %, $C11_b$ phase has the lower energy, and thus is the ground state of $MoSi_2$. With $x=8.3$ at. %, the two curves become almost isoenergetic, and we can expect the coexistence of two phases. When the concentration of Al increases to 16.7 at. %, E_{C40} becomes lower than E_{C11_b} by 368 meV. Correspondingly, the ground-state structure of $Mo(Si_{1-x},Al_x)_2$ changes from $C11_b$ to $C40$. Thus we demonstrate the phase transition of $Mo(Si_{1-x},Al_x)_2$ occurs when x goes from ~8.3 to ~16.7 at. %, which agrees with the experimental observation.[9]

Using of Murnaghan equation, the bulk modulus (B_0)'s of the two phases with different x are obtained and listed in Table II. B_0's of both phases decrease with the increase in the Al concentration. This can be attributed to the weaker chemical bonding of Al compared with Si. Also it has been suggested that phonon modes might lead to phase transitions.[17] We thus calculated A_{1g} and E_g phonon frequencies of $C11_b$ structure to understand the mechanism behind this $C11_b \rightarrow C40$ transition (shown in Table II). The substitution of Al softens both phonon modes and lifts the degeneration of E_g mode. Furthermore, there is no imaginary frequency with $x=16.7$ at. %. Thus the $C11_b$ is still a metastable structure for $Mo(Si_{1-x},Al_x)_2$ with high x values. This result indicates that phonon modes are not dominant factors in the doping-induced phase transition. This also drives us to investigate the origin of the phase transition on electronic structure rather than phonon modes.

TABLE II. The bulk modulus B_0 (Mbar) of $C11_b$ and $C40$ with different x. The optical phonon frequencies $\nu(cm^{-1})$ of $C11_b$ structure. Values in parenthesis are from Ref. 18.

	x (at. %)	0	8.3	16.7
B_0 (Mbar)	$C11_b$	2.07	2.03	2.02
	$C40$	2.02	1.99	1.95
$\nu(cm^{-1})$	E_g	440 (440)	437	426
			429	422
	A_{1g}	322 (325)	314	304

Figure 3 shows the density of states (DOS) of $C11_b$ and $C40$. The Fermi energies (E_F's) of both structures shift downwards with the increase in x. The effect of Al on the electronic structure transforms $MoSi_2$ with $C40$ structure from semiconductor to metal [Fig. 3(b)]. Near E_F, the DOS of both structures are mainly composed of d-bands but with different d-bands splitting. Such differences can be attributed to the different symmetries of these two phases. Based on the crystal field theory, the symmetry of $MoSi_2$ with $C11_b$ structure is D_{4h}, the d-bands reduces to $A_{1g} \oplus B_{1g} \oplus B_{2g} \oplus E_g$, and E_g subband lies nearest to the E_F. The symmetry of $C40$ structure is D_6^4, the d-bands reduces to $A_1 \oplus E_a \oplus E_b$, and A_1 is the subband which is nearest to the E_F. One should note that strictly speaking, the symmetry of system is broken due to the substitution of Al to Si, but as shown in Fig. 3, the profiles of DOS are similar and insensitive to x. Thus the analy-

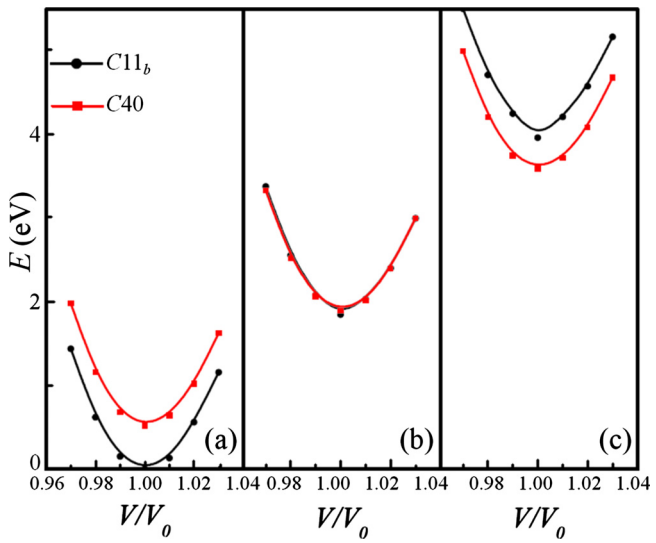

FIG. 2. (Color online) E vs V with different x: (a) 0 at. %, (b) 8.3 at. %, and (c) 16.7 at. %. The black circle and red (gray) square represent E_{C11_b} and E_{C40}, respectively. V_0 is the equilibrium volume of $Mo(Si_{1-x},Al_x)_2$. E_{C11_b} of $MoSi_2$ is set to zero.

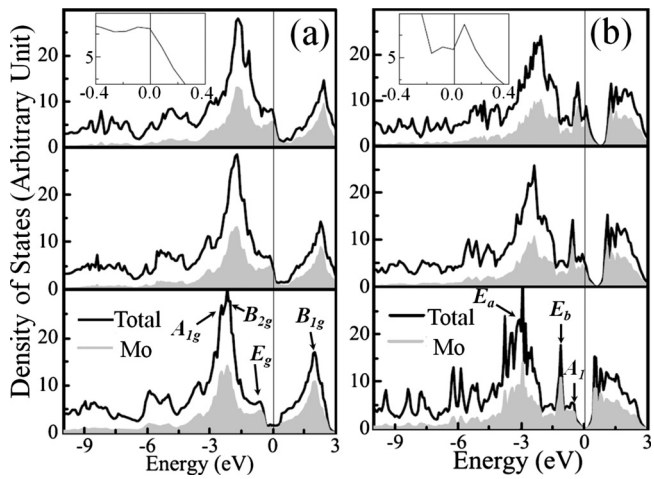

FIG. 3. DOS of $C11_b$ (a) and $C40$ (b) structure, respectively. From bottom to top, DOS of $x=0$ at. %, 8.3 at. %, and 16.7 at. %, respectively. The peaks of reduced subbands are indicated by arrows for both structures. Insets are the enlargement of the DOS near the E_F of both structures for $x=16.7$ at. %. E_F is set to zero, and represented by the vertical line.

sis on the symmetry still approximately holds.

Several studies have related the relative structural stability of alloys to DOS by, for example, the pseudogap effect[19,20] or the Jones-type analysis.[9,21–23] As an extension of previous models, we propose here a set of phenomenological criteria for predicting the structural stability using DOS. Namely, the system stability decreases as follows: (i) $n'(E_F)=0; n''(E_F)>0$, (ii) $n'(E_F)<0$, (iii) $n'(E_F)>0$, and (iv) $n'(E_F)=0; n''(E_F)<0$. where $n'(E_F)$, $n''(E_F)$ represent $(\partial n(E)/\partial E)|_{E_F}$ and $(\partial^2 n(E)/\partial E^2)|_{E_F}$, respectively. As shown in Fig. 3, when x is 8.3 at. %, $n'(E_F)$ of $C11_b$ and $C40$ are both negative and almost equal, thus energy difference is small and $Mo(Si_{1-x},Al_x)_2$ can be expected to have multiphases.[9] When $x=16.7$ at. %, the E_F of $C40$ structure lies at the local minimum between the A_1 and E_b subbands $[n''(E_F)>0]$. On the other hand, the E_F of $C11_b$ structure just lies at the local maximum of E_g subband, $[n''(E_F)<0]$. Thus $C40$ phase is more stable, and the ground-state structure of $Mo(Si_{1-x},Al_x)_2$ changes from $C11_b$ to $C40$. We thus reveal here the electronic origin that drives the phase transition: because of the different crystal field symmetry, d-bands of $C11_b$ and $C40$ structures reduce to different subbands. There are two subbands, A_1 and E_b, just below the E_F for $C40$ structure. Thus, DOS of $C40$ has a local minimum nearer to the E_F compared with that of $C11_b$. The substitution of Al 16.7 at. % changes the position of the E_F according to rigid band model, places the E_F of $C40$ at this minimum, and drives the observed phase transition.

These criteria are expected to be more general and can be used to guide the design of high-order $MoSi_2$-based alloy. We propose the ground-state structure control of $Mo(Si_{1-x},Al_x)_2$ by alloying with other transition metal elements, for example, to keep the $C11_b$ with high concentrations of Al by alloying with VII_B group elements, or to accelerate the phase transition at lower x by alloying with V_B group elements. To demonstrate the above prediction, We build four-order alloys by substituting Re and Nb to one of the Mo atoms in supercells of both $C11_b$ and $C40$, respectively. Due to the substitution of Nb, $C11_b$, and $C40$ co-exist in the alloy without Al, and in the case of $x=8.3$ at. %, $C40$ is already the ground state (E_{C40} is 190 meV lower). In contrast, alloying Re keeps $C11_b$ as the ground state till $x=16.7$ at. % (E_{C11_b} is favored by 114 meV). According to the electronic mechanism presented above, because the number of valence electrons of Nb is less than that of Mo, the E_F of $C40$ will shift to the local minimum between the A_1 and E_b subbands at relative lower x, and accelerate the phase transition. In the case of (Mo,Re) $(Si_{1-x},Al_x)_2$, the trend is opposite.

In conclusion, we investigated the detailed mechanism of the phase transition in $Mo(Si_{1-x},Al_x)_2$ using first-principles calculations. Based on the DOS and crystal field symmetry analysis, it was found that the phase transition is largely determined by the position of the Fermi level with respect to the local maximum of the subbands. We further demonstrate the feasibility of controlling the desired microscopic structure of $Mo(Si_{1-x},Al_x)_2$ by adding a quaternary component.

R. Chen and B. Shan would like to acknowledge the support from Program for New Century Excellent Talents in University (NCET) and National Natural Science Foundation of China (Grant No. 11004068). Calculations presented in this paper were carried out using the High Performance Computing Center experimental testbed in SCTS/CGCL (see http://grid.hust.edu.cn/hpcc).

[1]M. Fu and J. A. Sekhar, J. Am. Ceram. Soc. **81**, 3205 (1998).
[2]C. E. Ramberg and W. L. Worrell, J. Am. Ceram. Soc. **85**, 444 (2002).
[3]K. Tanaka, K. Nawata, H. Inui, M. Yamaguchi, and M. Koiwa, Intermetallics **6**, 607 (1998).
[4]L. F. Mattheiss, Phys. Rev. B **45**, 3252 (1992).
[5]M. Friák, M. Šob, and V. Vitek, Phys. Rev. B **68**, 184101 (2003).
[6]M. Alouani, R. C. Albers, and M. Methfessel, Phys. Rev. B **43**, 6500 (1991).
[7]X. Y. Zhang, W. Sprengel, T. E. M. Staab, H. Inui, and H.-E. Schaefer, Phys. Rev. Lett. **92**, 155502 (2004).
[8]X. Y. Zhang, W. Sprengel, K. Blaurock, A. A. Rempel, K. J. Reichle, K. Reimann, H. Inui, and H.-E. Schaefer, Phys. Rev. B **66**, 144105 (2002).
[9]D. Pankhurst, Z. Yuan, D. Nguyen-Manh, M.-L. Abel, G. Shao, J. Watts, D. Pettifor, and P. Tsakiropoulos, Phys. Rev. B **71**, 075114 (2005).
[10]K. Hagihara, T. Nakano, and Y. Umakoshi, Scr. Mater. **38**, 471 (1998).
[11]R. Mitra and V. V. Rama Rao, Mater. Sci. Eng., A **260**, 146 (1999).
[12]A. Stergiou and P. Tsakiropoulos, Intermetallics **5**, 117 (1997).
[13]Y. Liu, G. Shao, and P. Tsakiropoulos, Intermetallics **8**, 953 (2000).
[14]G. Kresse and J. Furthmuller, Phys. Rev. B **54**, 11169 (1996).
[15]J. P. Perdew and Y. Wang, Phys. Rev. B **45**, 13244 (1992).
[16]H. J. Monkhorst and J. D. Pack, Phys. Rev. B **13**, 5188 (1976).
[17]T. Tohei, A. Kuwabara, T. Yamamoto, F. Oba, and I. Tanaka, Phys. Rev. Lett. **94**, 035502 (2005), and references therein.
[18]C. M. Doland and R. J. Nemanich, J. Mater. Res. **5**, 2854 (1990).
[19]R. Yu, L. L. He, and H. Q. Ye, Phys. Rev. B **65**, 184102 (2002).
[20]J. Zou and C. L. Fu, Phys. Rev. B **51**, 2115 (1995).
[21]H. Jones, J. Phys. Radium **23**, 637 (1962).
[22]D. Nguyen-Manh, A. T. Paxton, D. G. Pettifor, and A. Pasturel, Intermetallics **3**, 9 (1995).
[23]D. A. Pankhurst, D. Nguyen-Manh, and D. G. Pettifor, Phys. Rev. B **69**, 075113 (2004).